Journal of Hazardous Materials 311 (2016) 246–253

Contents lists available at ScienceDirect

Journal of Hazardous Materials

journal homepage: www.elsevier.com/locate/jhazmat

Double-Barrier mechanism for chromium immobilization: A quantitative study of crystallization and leachability

Changzhong Liao[a,b,1], Yuanyuan Tang[c,1], Chengshuai Liu[a,d,*], Kaimin Shih[b], Fangbai Li[a]

[a] Guangdong Key Laboratory of Agricultural Environment Pollution Integrated Control, Guangdong Institute of Eco-Environmental and Soil Sciences, Guangzhou 510650, PR China
[b] Department of Civil Engineering, The University of Hong Kong, Pokfulam Road, Hong Kong SAR, PR China
[c] School of Environmental Science and Engineering, South University of Science and Technology of China, Shenzhen 518055, PR China
[d] State Key Laboratory of Environmental Geochemistry, Institute of Geochemistry, Chinese Academy of Sciences, Guiyang 550009, PR China

HIGHLIGHTS

- The glass-ceramic samples were proven to be excellent in immobilizing Cr.
- Glass-ceramic was successfully synthesized in CaO-MgO-SiO_2-Al_2O_3 -Cr_2O_3 system.
- Both crystalline and glass phases were quantified by Rietveld quantitative XRD.
- The partitioning ratio of Cr into spinel in the glass-ceramic can be up to 90%.

GRAPHICAL ABSTRACT

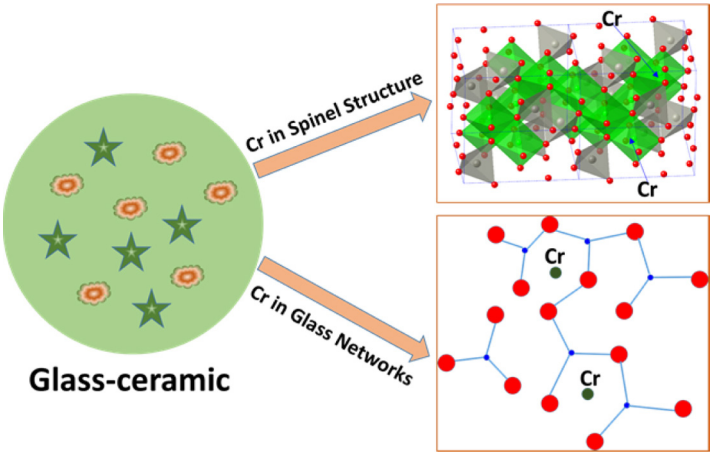

Schematic illustration of chromium incorporating in the glass-ceramic matrix. Most chromium contents are incorporated into spinel structure where the residual chromium are resided in the glass networks.

ARTICLE INFO

Article history:
Received 18 November 2015
Received in revised form 7 March 2016
Accepted 7 March 2016
Available online 9 March 2016

Keywords:
Glass-ceramic
Spinel
Chromium immobilization
Rietveld quantitative XRD
Leaching performance

ABSTRACT

Glass-ceramics are well known for the excellent combination properties provided by their components, a glassy matrix and crystalline phases, and have promising applications in the immobilization and detoxification of solid waste containing toxic metals. Glass-ceramic products were successfully synthesized in CaO-MgO-SiO_2-Al_2O_3 -Cr_2O_3 system. Two key measures – partitioning ratio of Cr in the spinel and Cr leaching ratio – were used to investigate the mechanism of Cr immobilization in the glass-ceramic products. The results of powder X-ray diffraction revealed that both spinel and diopside were major crystalline phases in the products. The value of x in the $MgCr_xAl_{2-x}O_4$ spinel was highly related to the amount of Cr_2O_3 added to the glass-ceramic system. As Cr_2O_3 content increased, the proportion of spinel phase increased, while that of glass phase decreased. The partitioning ratio of Cr in spinel phase was about 70% for 2 wt.% Cr_2O_3, and increased to 90% when loaded with 10 wt.% of Cr_2O_3. According to the results of the

* Corresponding author.
E-mail address: csliu@soil.gd.cn (C. Liu).
[1] These authors contributed equally to this manuscript.

http://dx.doi.org/10.1016/j.jhazmat.2016.03.020

prolonged toxicity characteristic leaching procedure, the Cr leaching ratio decreased with the increase of Cr partitioning ratio into the spinel phase. The findings of this study clearly indicate that glass-ceramic formed by spinel structure and residual glass successfully immobilized Cr.

1. Introduction

Millions of tons of chromium (Cr) slag worldwide have been dumped and spread over large areas without receiving appropriate treatment at industrial sites. This has caused severe environmental problems in many countries [1]. The continuous leaching of hexavalent Cr, Cr(VI), from Cr slag can seriously contaminate the surrounding environment, such as soil, sediment, underground water, and surface water [2–4]. For example, the Cr concentration of soil and sediment at contaminated source sites may be very high—in some cases exceeding 10,000 mg kg^{-1} [5]. Environmental Cr contamination poses a serious threat to humans, plants and animals. Therefore, an effective method of treating Cr slag is urgently required to protect the environment and human health. In the environment, Cr(III) and Cr(VI) are the two common oxidation states. Generally, Cr(VI) is much more mobile and more toxic than Cr(III) [6,7]. In addition to the hazards caused by their strong oxidation properties, chromate ions (CrO_4^{2-}) pass through cellular membranes many orders of magnitude faster than do Cr(III) species, resulting in much greater toxic effects on cells [8,9]. All Cr waste must be treated properly before being reused or released to the environment. Stabilization/solidification (S/S) treatment can reduce the mobility of heavy metals by converting hazardous waste into chemically stable solids [10–12]. However, S/S processes have rarely been successfully used to prevent the leaching of toxic metals in acidic environments [12].

Deriving excellent properties from the combination of a glassy matrix and embedded crystalline phases, [13] marketable glass-ceramics have been prepared from blast-furnace slag, fly ash, sludge, and glass cullet. [14–17] Converting waste to useful glass-ceramics is considered a promising method of protecting the environment and promoting sustainable development. Glass-ceramics are usually produced from the controlled crystallization and devitrification of glass [18], and nucleation processes are critical throughout their fabrication. [19–21] The major components of Cr slag have been shown to be calcium (Ca), magnesium (Mg), silicon (Si), and aluminum (Al) [7], which make up the glass-ceramic matrix. In addition, Cr_2O_3 has been found to be an effective crystallization nucleant during glass production in a quartz sand-dolomite-magnesite system [22] and an SiO_2-Al_2O_3-CaO-Fe_2O_3 system [23]. Barbieri et al. [24] also found that $MgCr_2O_4$ spinel crystallites act as heterogeneous nucleation sites for diopside and anorthite phases after the addition of Cr_2O_3 to an SiO_2-Al_2O_3-CaO-MgO system. However, the above work did not point out the distribution of Cr in glass-ceramic products nor the formed Cr-bearing phases. To ensure the safe and effective reuse of Cr slag as marketable glass-ceramics, Cr should be immobilized to ensure that very little can leach out when the glass-ceramic products are used in the environment. Based on the major reported components of Cr waste, a simulated Cr slag with the system of CaO-MgO-SiO_2-Al_2O_3-Cr_2O_3 was designed in this study [25]. Previous research has shown the promising performance of spinel structures in hosting hazardous metals, and that the metal leachability of the spinel phase is several orders lower than that of metal oxides [26–29]. Therefore, the reported formation of Cr spinel in the CaO-MgO-SiO_2-Al_2O_3-Cr_2O_3 system [25] is expected to greatly facilitate the immobilization of Cr in glass-ceramic products.

Crystalline-phase parameters have been reported to be one of the most important factors affecting the properties of glass-ceramics [30,31], and the formation of crystalline phases is acknowledged to be critical to metal stabilization in glass-ceramics [18,32,33]. Therefore, it is essential to identify the structure and quantify the crystalline phases in glass-ceramic products. Rietveld quantitative X-ray diffraction (QXRD) analysis with spiking a standard reference material (such as Al_2O_3 or CaF_2) is a powerful tool to quantify compositions of both crystalline and amorphous phases in the glass-ceramic samples [34–39]. In the CaO-MgO-SiO_2-Al_2O_3-Cr_2O_3 system mentioned above, the Cr-spinel is expected to form a solid solution due to the complexity of the system [40]. The precise chemical compositions, especially the distribution of hazardous metals between crystalline and glass phases, are highly beneficial to discuss the capacity of glass-ceramics to accommodate the hazardous metals. Transmission electron microscopy-energy dispersive X-ray spectroscopy (TEM-EDX) can be used to obtain detailed information at nano level without interference from other areas [41], ensuring that accurate data are acquired from both crystal and residual glass. Thus, it is powerful to determine the chemical composition of the spinel solid solution in the glass-ceramic matrix.

In this study, simulated Cr slag with varying Cr_2O_3 content in a CaO-MgO-SiO_2-Al_2O_3-Cr_2O_3 system was treated to synthesize glass-ceramic products. To obtain the precise chemical compositions of the crystals in the glass-ceramics, the spinel crystals were probed by the TEM-EDX. The phase components were qualitatively identified by powder XRD, and quantitatively determined by Rietveld quantitative phase analysis with spiking standard reference. A prolonged leaching procedure was also carried out to examine the stabilization of Cr in the glass-ceramics products. Two measures – the Cr partitioning ratio (PR) and the Cr leaching ratio – were used to investigate Cr distribution in the glass-ceramic matrix and the extent of the immobilization of Cr in the glass-ceramic products.

2. Materials and methods

2.1. Preparation of Cr-bearing glass-ceramics

To simulate common Cr-containing slag, a mixture of CaO, MgO, SiO_2, Al_2O_3, and Cr_2O_3 was prepared. The chemical composition of the starting mixture (Table 1) was near the eutectic point of the $CaMgSi_2O_6$-$CaAl_2Si_2O_8$ pseudo-binary phase Diagram [25] to give the lowest possible melting temperature in the final CaO-MgO-SiO_2-Al_2O_3-Cr_2O_3 system. A mixture of reagent-grade oxides (MgO, SiO_2, Al_2O_3, and Cr_2O_3) and calcium carbonate ($CaCO_3$) with about

Table 1
Chemical compositions of the simulated chromium-containing slag (in wt.%) with different Cr_2O_3 contents in the starting materials.

Sample Name	Chemical Compositions (wt.%)				
	MgO	CaO	SiO_2	Al_2O_3	Cr_2O_3
P2	11.62	23.02	49.34	14.02	2.00
P4	11.86	22.43	48.06	13.66	4.00
P6	12.10	21.83	46.78	13.30	6.00
P8	12.34	21.23	45.50	12.93	8.00
P10	12.59	20.63	44.22	12.57	10.00

50 g in total were well-homogenized by mortar grinding. The mixture was melted at 1450 °C for 3 h in a high-temperature furnace (LHT 02/16 LB, LBR, Nabertherm Inc.), then immediately poured into an alumina crucible and cooled to room temperature in the air.

2.2. Analysis and characterization of Cr-bearing glass-ceramics

One set of product samples was treated by mechanical thinning, followed by ion-beam milling (Fischione Model 1010 Ion Beam Mill). The treated samples were then characterized by TEM, selected area electron diffraction (SAED), and EDX analysis performed on a FEI Tecnai G220 S-TWIN at 200 kV. The other samples were polished and characterized by SEM and EDX spectral analysis using a Hitachi S–3400 N SEM operating in variable-pressure mode. The phases of the products were characterized by powder XRD. The step-scanned XRD patterns for individual powder samples were collected using a Bruker D8 Advance X-ray powder diffractometer (Mannheim, Germany) equipped with a Cu Kα1,2 X-ray radiation source (40 kV, 40 mA) and a LynxEye detector. The 2θ scanning range was 10–110°, and the step size was 0.02°, with a scanning speed of 2 s step^{-1}. The phases were qualitatively identified by matching the powder XRD patterns with equivalent patterns retrieved from the standard powder diffraction database of the International Centre for Diffraction Data (ICDD PDF-2, Release 2008; Pennsylvania, U.S.). The product phases were all quantitatively analyzed using Topas 4–2 (Bruker, Mannheim, Germany), a tool based on Rietveld refinement. Refinement analysis with 20 wt.% CaF_2 as a standard reference was carried out to quantify the phase compositions (including the crystalline and amorphous content) of the samples.

The Cr K-edge X-ray absorption near edge structure (XANES) spectra were collected in fluorescent mode using a Lytle detector at beamline 16A of the National Synchrotron Radiation Research Center (NSRRC), Hsinchu, Taiwan. The spectra of pure chemicals Cr_2O_3 and CrO_3 were also measured to serve as the references of Cr(III) and Cr(VI) oxidation states. The energy of the monochromator was calibrated using the Cr K-edge at 5989 eV. Processing and analysis of XANES spectra was carried out using ATHENA (Demeter software package version 0.9.18) [42].

2.3. Leaching performance of glass-Ceramic products

The leachability of each sintered sample was tested using a modified version of the toxicity characteristic leaching procedure (TCLP) developed by the U.S. Environmental Protection Agency, with a pH 2.9 acetic acid solution (extraction fluid #2) as the leaching fluid. Each leaching vial was filled with 5 mL of TCLP extraction fluid and 0.25 g of powder, and the vials were rotated end over end at 30 rpm for agitation periods of 3 h to 25 d. At the end of each agitation period, the leachates were filtered with syringe filters (0.22 μm, nylon) into clean centrifuge tubes and reserved for analysis. The pH of the samples was measured, and the concentrations of the predominant metals in the filtrate were derived using an inductive coupled plasma-atomic emission spectrometer (Perkin-Elmer Optima 8000).

3. Results and discussion

3.1. Identification of phases and chemical composition of solid spinel solution

Glass-ceramic products were obtained in a simulated Cr-containing CaO-MgO-SiO_2-Al_2O_3-Cr_2O_3 slag system by high-temperature melting. The XRD results (Fig. 1a) revealed two crystalline phases in the glass-ceramic products: spinel and diopside (normal formula: $CaMgSi_2O_6$). However, phase composition was found to differ according to Cr_2O_3 content. A crystalline phase with a spinel structure was clearly detected in the glass-ceramics produced using 2 wt.% of Cr_2O_3, whereas the diopside signal for this system was very weak. With the continuous addition of Cr_2O_3 to the reaction system, both a spinel phase and a diopside phase were observed in the glass-ceramic products, with a clear increase in peak intensity in each case. The XRD patterns in Fig. 1b enable further comparison of the predominant peaks of diopside and spinel within the 2θ range of 29.0–31.0° and 35.0–37.0°, respectively. The patterns clearly demonstrate that both diopside and spinel peak intensity increased with the weight percentage of Cr_2O_3.

In addition, as Cr_2O_3 content increased, the 2θ position of the spinel peaks was observed to shift from a higher to a lower degree, while smaller changes were observed in the diopside peaks (Fig. 1b). This shift in the spinel phase peaks may have been due to changes in the lattice parameters of the spinel structure. When the system contained various proportions of MgO, Cr_2O_3, and Al_2O_3, a solid spinel solution was formed during the melting process, with a chemical formula of $MgCr_xAl_{2-x}O_4$ [40]. The value of x differed according to the chemical composition of the raw materials. Changes in x altered the lattice parameters of the spinel crystal, causing the diffraction peaks to shift. Rietveld refinement was applied to the obtained XRD patterns. The lattice parameters of the spinel phase are shown in Table S1 (Supporting information). The lattice parameters clearly increased with the Cr_2O_3 content of the starting mixture, indicating that Cr incorporation into the spinel phase was affected by the initial level of Cr_2O_3. To determine the chemical composition of the solid spinel solution (specifically the value of x) in the obtained glass-ceramic products, TEM-EDX was used to detect the signals from each element (as shown in Fig. 2). As shown in Fig. 2a, two key areas (areas 1 and 2) were selected near the edge of the crystal grains and the glass, respectively. The SAED pattern shown in Fig. 2b further demonstrates that area 1 was composed of spinel crystals. The chemical composition of the spinel crystals was also obtained in grain areas similar to area 1, located at the edge of the thin sample without overlap with the glass phase. Figs. 2c and d illustrate the significantly different element compositions of areas 1 and 2, as measured by TEM-EDX. Area 1 was composed mainly of Mg, Al, Cr, and O, while Si and Ca made up the majority of area 2. The results confirm that area 1 was located on a spinel grain with a chemical formula of $MgCr_xAl_{2-x}O_4$, whereas area 2 was located on the matrix, and was composed mainly of Si- and Ca-containing minerals. The precise element composition of the spinel crystals were determined accordingly. The average values were obtained by statistically analyzing the composition of the elements detected in five spinel grains. The results are shown in Table S2 (Supporting information). The atomic percentage of Cr in the solid solution $MgAl_{2-x}Cr_xO_4$ increased with the continuous addition of Cr_2O_3 to the starting raw materials, whereas those of Al decreased. As the radius of the Cr ions was larger than that of the Al ions, the lattice parameters of the spinel phase increased due to the continuous incorporation of Cr to substitute for Al. The increase in the lattice parameters of the solid spinel solution was confirmed by the results of Rietveld refinement analysis of the XRD patterns obtained for the glass-ceramic products (Table S1 in Supporting information).

For further comparison and confirmation, SEM-EDX was used to conduct element analysis. The microstructures of the glass-ceramics and the elements detected in selected areas (“a” and “b”) are shown in Fig. S1 (Supporting information), in which the light-colored areas represent crystalline phases and the gray areas represent residual glass. The EDX spectra show that elements such as Mg, Al, Cr, and Si all had very strong signals in both area “a” and area “b”. As the spinel grain in area “a” had a chemical for-

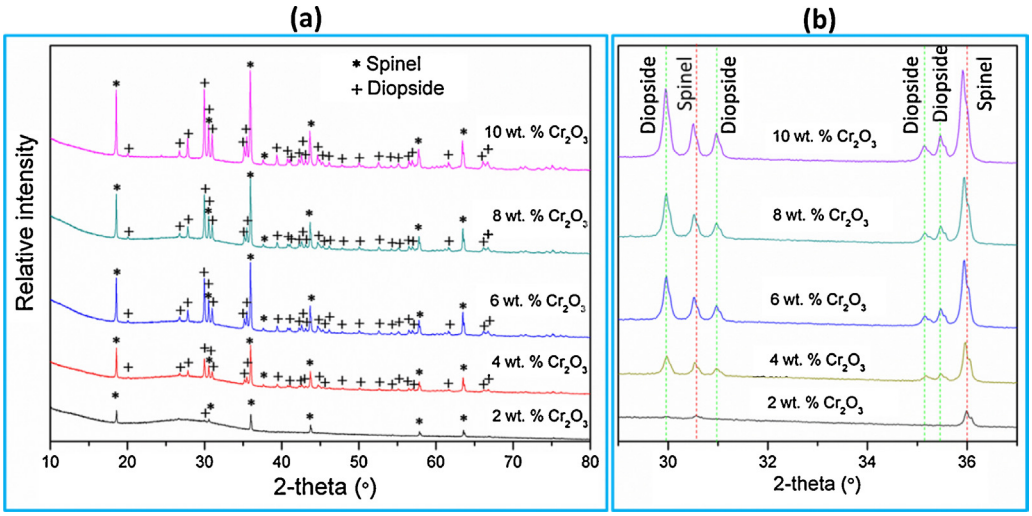

Fig. 1. (a) XRD patterns for glass-ceramics produced from starting mixtures containing different proportions of Cr_2O_3; (b) Comparison of the major peaks for spinel and diopside, showing a peak shift for the spinel phase but no evidence of a peak shift for diopside.

mula of $MgCr_xAl_{2-x}O_4$, the spinel crystal was assumed to contain little Si. However, a strong Si peak was observed in area "a", similar to that in area "b" (Fig. S1, Supporting information), indicating signal interference caused by residual glass and the inaccuracy of the SEM-EDX measurements of chemical composition. Therefore, these results further confirm that compared with SEM-EDX, TEM-EDX provides a more accurate and effective means of obtaining the chemical composition of spinel crystal in glass-ceramics.

3.2. Quantification of Cr-Incorporation mechanisms

After the XRD patterns had been subjected to Rietveld refinement with standard reference materials, the weight fractions of

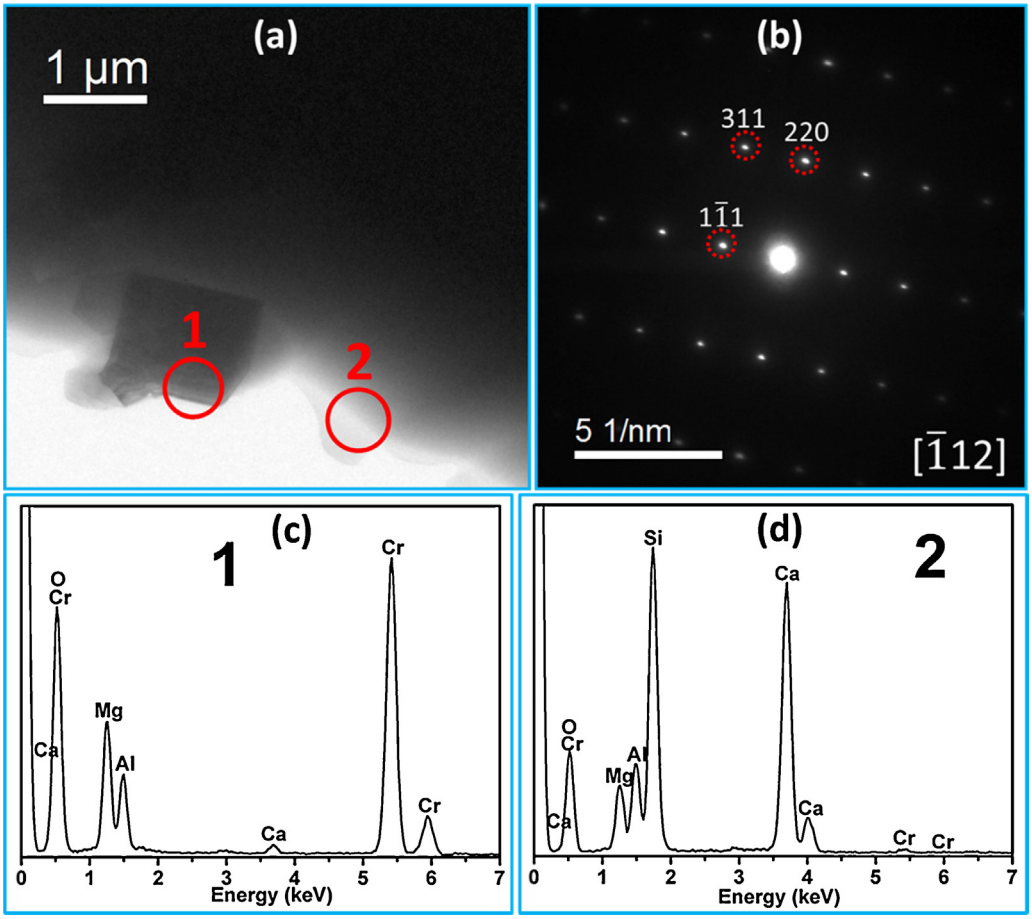

Fig. 2. (a) Bright-field TEM image of the glass-ceramics with a starting mixture containing 2 wt.% of Cr_2O_3; (b) SAED results to confirm the spinel crystal; TEM-EDX spectra for the crystal (area 1) (c) and the residual glass (area 2) (d).

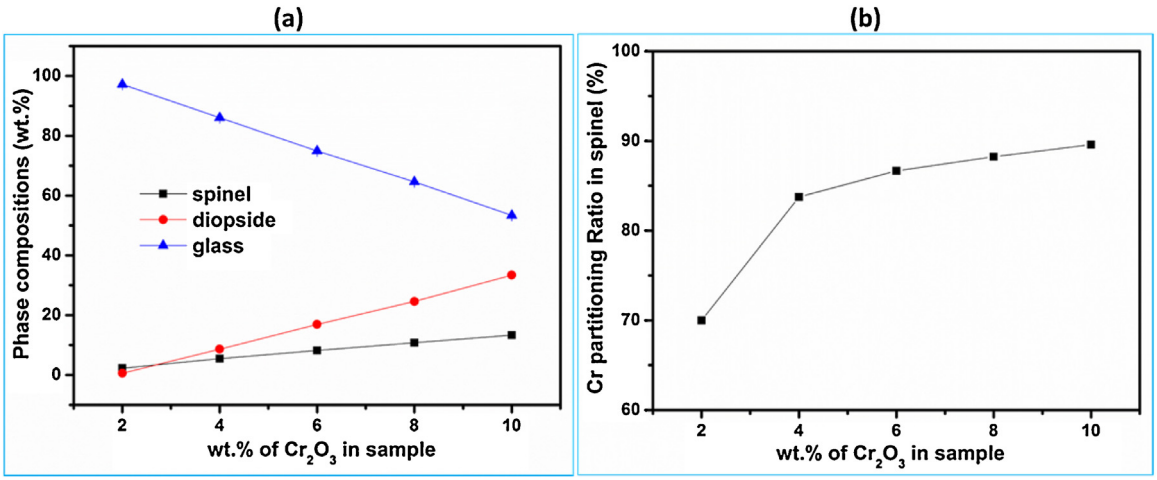

Fig. 3. (a) Quantitative composition of spinel, diopside, and glass in the as-formed glass-ceramic system with different percentages of Cr_2O_3, and (b) Partitioning ratio (PR) of Cr in the spinel phase. CaF_2 was used as an internal standard to quantify the amorphous phase(s) in the system when carried out Rietveld quantitative XRD analysis.

the components (including crystalline and amorphous phases) of the glass-ceramic products were obtained. The results are shown in Fig. 3. When 2 wt.% of Cr_2O_3 was added to the system, the glass phase(s) made up more than 95% of the products. With a further increase in Cr_2O_3 content to 10 wt.%, the weight percentage of the glass phase(s) decreased linearly, finally reaching approximately 50%. In contrast, the crystalline phase(s) continued to grow, as illustrated in Fig. 3a. The weight percentage of the spinel phase increased from about 2% to around 10%, and that of the diopside phase ultimately exceeded 30% after adding 10 wt.% of Cr_2O_3 to the system. These results indicate that increasing Cr_2O_3 content can enhance crystallization in a CaO-MgO-SiO_2-Al_2O_3-Cr_2O_3 system. Similarly, other studies have revealed that Cr_2O_3 in an initial glass system may act as a heterogeneous nucleation site for the crystallization of diopside [24,43] and increase the formation of diopside [44].

As spinel is the dominant Cr-hosting crystalline phase, it was crucial to study the distribution of Cr between the spinel and other phases in the glass-ceramics products. The distribution of Cr was examined using a "partitioning ratio (PR)" index, and it was defined as the ratio of the weight of Cr_2O_3 incorporated into the spinel phase to the total Cr_2O_3 used in the mixture. The equation can be described as follows,

$$\mathrm{PR} = \frac{wt.\%\mathrm{of}MgCr_xAl_{2-x}O_4 \times \frac{\mathrm{MWof}Cr_xO_{1.5x}}{\mathrm{MWof}MgCr_xAl_{2-x}O_4}}{wt.\%\mathrm{of}Cr_2O_3\mathrm{insample}} \quad (1)$$

where the chemical formula of $MgCr_xAl_{2-x}O_4$ is determined by TEM-EDX, the wt.% of $MgCr_xAl_{2-x}O_4$ is determined by XRD quantification analysis with a standard reference, and MW indicates molecular weight. A PR of 100% denotes the complete incorporation of Cr into the spinel phase; a PR of 0% indicates that no Cr has been incorporated into the spinel. As shown in Fig. 3b, the PR of Cr in the spinel phase continuously increased with the amount of Cr_2O_3 added to the system. When 2 wt.% of Cr_2O_3 was added to the glass-ceramics system, approximately 70% of the Cr was incorporated into the crystalline spinel phase, while 30% remained in the residual glass matrix. However, when the content of Cr_2O_3 was 4 wt.%, the amount of Cr incorporated into the spinel phase increased significantly, from 70% to 85%. With a further increase in Cr_2O_3 content, the PR of Cr in the spinel continued to increase, but at a lower rate. PR reached its maximum value of approximately 90% when the largest proportion of Cr_2O_3 (10 wt.%) was added. This increase in PR may be related to the large octahedral site preferential energy of Cr in glass structures, leading to the formation of Cr-concentrated spinel [45,46]. These results indicate that most of the Cr element was incorporated into the spinel phase, with only a small fraction dispersed in the residual glass and/or the diopside phase. In addition, the element-mapping profile for glass-ceramics with 10 wt.% Cr_2O_3 clearly shows that the Cr element was concentrated in the spinel crystal and that the residual glass was rich in Si, Ca, and Al (Fig. S2, Supporting information). The microstructure depicted in SEM image in Fig. S2 (Supporting information) shows that spinel crystals were embedded in the glass matrix. This created a double barrier for Cr, with the Cr spinel as the first barrier and residual glass as the second.

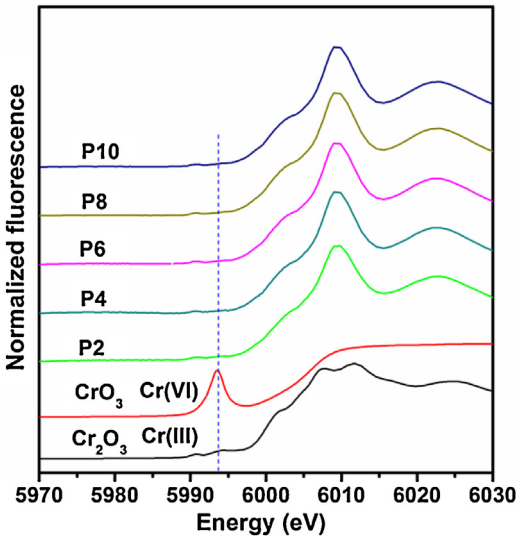

Fig. 4. Cr K-edge XANES spectra of P2, P4, P6, P8, P10 and reference compounds containing Cr(III) and Cr(VI) (Cr_2O_3 for Cr(III) and CrO_3 for Cr(VI)). P2, P4, P6, P8 and P10 are corresponding to the glass-ceramic matrices with Cr_2O_3 contents of 2, 4, 6, 8, 10 wt.%, respectively.

3.3. Performance of Cr immobilization in glass-Ceramic products

As particular emphasis is placed on removing Cr(VI) during the treatment of Cr slag, the transformation of Cr(VI) to Cr(III) is always considered an important measure of the efficacy of Cr-waste disposal. Therefore, the valence state of Cr in the as-formed glass-ceramics was also investigated in this study. Fig. 4 shows the Cr K-edge XANES spectra of P2, P4, P6, P8, P10 and reference com-

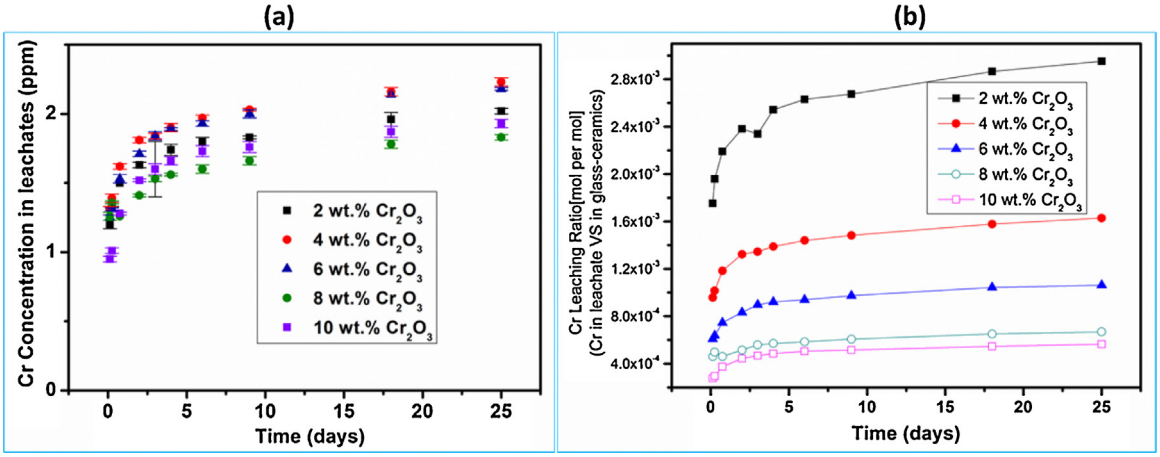

Fig. 5. (a) Concentrations of Cr in leachates of the glass-ceramic products synthesized with different proportions of Cr_2O_3 in their starting mixtures, and (b) normalized Cr leaching ratio with respect to Cr_2O_3 content.

pounds containing Cr(III) and Cr(VI) (Cr_2O_3 for Cr(III) and CrO_3 for Cr(VI)). In the Cr k-edge XANES spectra, there is a strong pre-edge peak in the Cr(VI)-bearing compounds. However, this strong pre-edge peak is absent in the Cr(III)-containing compounds [47]. Thus, it can be used to identify the existence of Cr(VI) species in the samples. Comparing the Cr k-edge XANES spectra of all glass-ceramic products and reference compounds containing Cr(III) and Cr(VI), it can be seen that no evidence of Cr(VI) was observed in the obtained glass-ceramic products. Therefore, it is reasonable to claim that the Cr(III) in the original materials did not oxidize into Cr(VI) after glass-ceramic fabrication. In a study of the solubility of Cr_2O_3 in a similar system, Barbieri et al. [24] also found that Cr(III) was the only oxidation state. In other studies, the results of X-ray absorption near edge structure calculations have indicated that Cr(III) is in a stable state at temperatures higher than 1100 °C, whereas Cr(VI)-bearing forms (such as CrO_4^{2-}) are decomposed and reduced to Cr(III) under the same conditions [48]. In the current study, the absence of Cr(VI) suggested that Cr contents in synthesized glass-ceramic products are in forms of a non-toxic state, Cr(III).

To further investigate the stabilization of the immobilized Cr in the glass-ceramic products, the Cr leachability of the as-formed products was monitored through a prolonged acid leaching test. As illustrated in Fig. 5a, the original concentrations of Cr in the leachates were not substantially different (differences within 0.4 ppm). Cr concentration in the leachates increased quickly during the first 5 days, then remained relatively stable with increasing leaching time. When 2 wt.% of C_2O_3 was added to the starting mixture, approximately 1.74 mg/L of Cr had been leached from the glass-ceramics by the 4th day, and this value had reached 2.02 mg/L by the end of the leaching experiment. Despite the similar Cr concentrations of the leachates produced from glass-ceramics containing different amounts of Cr_2O_3, the highest Cr concentration was approximately 2 ppm. This value is lower than the criteria (5 ppm) for hazardous solid waste [49], despite the use of fine power in our leaching experiment (as compared with the bulk samples used in standard tests) [50].To compare the effects of Cr_2O_3 content on Cr stabilization in glass-ceramic products, the following Cr leaching ratio was introduced,

$$Cr_{LR} = \frac{\frac{C \times V \times 10^{-6}}{MWofCr}}{2 \times \frac{SW \times wt.\%ofCr_2O_3 insample}{MWofCr_2O_3}} \quad (2)$$

where C (mg/L) is the measured Cr concentration in the leachates, V (mL) is the extraction-fluid volume, SW (g) is the total sample weight used in the leaching experiment, "wt.% of Cr_2O_3 in the sample" denotes the percentage of Cr_2O_3 in the glass-ceramics starting mixture, and MW represents molecular weight.

As shown in Fig. 5b, the glass-ceramics with 2 wt.% of Cr_2O_3 had the highest Cr leaching ratio, whereas 10 wt.% of Cr_2O_3 yielded the lowest Cr leaching ratio. Increasing the Cr_2O_3 content of the starting mixture reduced the Cr leaching ratio of the corresponding glass-ceramic products. The Cr leaching ratio clearly decreased as the spinel phase grew and the PR of Cr in the spinel phase increased. This decrease in Cr leachability further confirmed the excellent performance of the spinel phase in immobilizing hazardous Cr ions. The superiority of the spinel structure as an agent of metal immobilization has also been reported by researchers exploring stabilization mechanisms for hazardous metals (Ni, Cu, Zn, etc.) in Al-rich and Fe-rich systems [26–29]. In the researches of Shih and Tang, they used a prolonged acid leaching test (pH 2.9) to demonstrate the superiority of the spinel structure in immobilizing hazardous metals, compared with other metal-bearing materials. That is one of the reasons why the acid leaching test was also used to demonstrate the enhanced durability of the glass-ceramic products in this study. In addition to the leaching of Cr from the glass-ceramics, the leachability of other major constituents (Ca, Al, Mg and Si) was analyzed, and the results are shown in Fig. S3 (Supporting information). All of the above ions were detected by a decrease in the concentration of the leachates of sintered glass-ceramics with an increase in original Cr_2O_3 from 2 wt.% (Fig. S3a) to 10 wt.% (Fig. S3b). In addition, comparison of the molar concentrations revealed that Ca had the highest leachability and Al had the lowest leachability. The molar concentrations of Si in the leachates of glass-ceramics were higher than those of Mg with 2 wt.% of Cr_2O_3, but similar when the glass-ceramics were prepared with 10 wt.% of Cr_2O_3.

3.4. Potential environmental implications

With increasing industrial demand for Cr compounds, more and more Cr-bearing wastes, such as slag from electronic plating, tanneries, and chrome-ore mining, are generated each year. Most of these wastes are directly deposited by storage or landfill, and thus cause serious environmental problems. Chromium ore processing residue contains large amounts of Cr(VI), which are released to the surrounding environment after long periods of storage, posing a hazard to ground water. Thereby, an appropriate treatment method enabling the safe disposal of large volumes of Cr-bearing waste is urgently needed. The proposed waste-to-resource strategy is expected to offer a promising solution. An ideal waste-to-resource

strategy results in zero waste, as the industrial by-product receives other useful applications. Our experimental results demonstrated that with thermal treatment, Cr in simulated Cr slag with a phase structure of CaO-MgO-SiO_2-Al_2O_3-Cr_2O_3 can be efficiently incorporated into spinel, yielding a glass-ceramic product that provides a double barrier to the mobilization of Cr. In solid $MgCr_xAl_{2-x}O_4$ spinel solution with a specific element composition and crystalline and amorphous phases quantified by XRD and TEM-EDX, the PR of Cr in the spinel phase increased when more Cr_2O_3 was added to the system, and the Cr leaching ratio decreased. This further indicates the potential of the proposed technology to stabilize large volumes of Cr, enabling the reuse of slag as glass-ceramic products. Overall, the results of our empirical tests of a novel double-barrier method of Cr immobilization and our quantitative analysis of the potential stabilization mechanisms in reusable glass-ceramic products suggest that the proposed strategy offers an environmentally safe method of treating large volumes of Cr slag.

Availability of supporting information

Three tables and three figures illustrating the raw material compositions, the refinement results, the supplementary SEM results, and the leaching results are available free of charge online at http://pubs.acs.org.

Acknowledgments

The authors would like to thank Frankie Y. F. Chan for his help with the TEM experiments and other advice. This study was funded by the National Natural Science Foundation of China (41171364), the Guangdong Natural Science Foundation of China (S2011030002882), the Science and Technology Planning Project of Guangzhou, China (2013J4500024), the One Hundred Talents Programme of the Chinese Academy of Sciences, the General Research Fund Scheme of the Research Grants Council of Hong Kong (715612, 17206714) and HKU Strategic Research Themes on Clear Energy and Earth as a Habitable Planet.

Appendix A. Supplementary data

Supplementary data associated with this article can be found, in the online version, at http://dx.doi.org/10.1016/j.jhazmat.2016.03.020.

References

[1] Y. Gao, J. Xia, Chromium contamination accident in China: viewing environment policy of China, Environ. Sci. Technol. 45 (20) (2011) 8605–8606.
[2] C.J. Cheng, T.H. Lin, C.P. Chen, K.W. Juang, D.Y. Lee, The effectiveness of ferrous iron and sodium dithionite for decreasing resin-extractable Cr(VI) in Cr(VI)-spiked alkaline soils, J. Hazard. Mater. 164 (2009) 510–516.
[3] K. Kim, J. Kim, A.D. Bokare, W. Choi, H.I. Yoon, J. Kim, Enhanced removal of hexavalent chromium in the presence of H_2O_2 in frozen aqueous solutions, Environ. Sci. Technol. 49 (18) (2015) 10937–10944.
[4] A.R. Wadhawan, A.T. Stone, E.J. Bouwer, Biogeochemical controls on hexavalent chromium formation in estuarine sediments, Environ. Sci. Technol. 47 (15) (2013) 8220–8228.
[5] T.K. Tokunaga, J. Wan, A. Lanzirotti, S.R. Sutton, M. Newville, W. Rao, Long-term stability of organic carbon-stimulated chromate reduction in contaminated soils and its relation to manganese redox status, Environ. Sci. Technol. 41 (2007) 4326–4331.
[6] N.H. Hsu, S.L. Wang, Y.C. Lin, D. Sheng, J.F. Lee, Reduction of Cr(VI) by crop-residue-derived black carbon, Environ. Sci. Technol. 43 (2009) 8801–8806.
[7] K. Pillay, H. Von Blottnitz, J. Petersen, Ageing of chromium(III)-bearing slag and its relation to the atmospheric oxidation of solid chromium(III)-oxide in the presence of calcium oxide, Chemosphere 52 (10) (2003) 1771–1779.
[8] A.G. Levis, V.E.R.A. Bianchi, Mutagenic and cytogenetic effects of chromium compounds, in: In Biological and Environmental Aspects of Chromium, Elsevier, Amsterdam, 1982, pp. 171–208.
[9] D.E. Kimbrough, Y. Cohen, A.M. Winer, L. Creelman, C. Mabuni, A critical assessment of chromium in the environment, Crit. Rev. Environ. Sci. Technol. 29 (1) (1999) 1–46.
[10] Y.L. Chen, M.S. Ko, Y.C. Lai, J.E. Chang, Hydration and leaching characteristics of cement pastes made from electroplating sludge, Waste Manage. 31 (6) (2011) 1357–1363.
[11] A.C. Sophia, K. Swaminathan, Assessment of the mechanical stability and chemical leachability of immobilized electroplating waste, Chemosphere 58 (1) (2005) 75–82.
[12] C.T. Li, W.J. Lee, K.L. Huang, S.F. Fu, Y.C. Lai, Vitrification of chromium electroplating sludge, Environ. Sci. Technol. 41 (8) (2007) 2950–2956.
[13] A. Niyompan, S. Phumas, R. Tipakontitikul, T. Tunkasiri, Phase formation, microstructure and electrical properties of mica glass-ceramics containing Cr_2O_3 produced by heat treatment, Ceram. Int. 39 (2013) S427–S431.
[14] A.A. Francis, Crystallization kinetics of magnetic glass–ceramics prepared by the processing of waste materials, Mater. Res. Bull. 41 (6) (2006) 1146–1154.
[15] K.C. Vasilopoulos, D.U. Tulyaganov, S. Agathopoulos, M.A. Karakassides, J.M.F. Ferreira, D. Tsipas, Bulk nucleated fine grained mono-mineral glass-ceramics from low-silica fly ash, Ceram. Int. 35 (2) (2009) 555–558.
[16] J. Zhang, W. Dong, J. Li, L. Qiao, J. Zheng, J. Sheng, Utilization of coal fly ash in the glass–ceramic production, J. Hazard. Mat. 149 (2) (2007) 523–526.
[17] E. Bernardo, J. Doyle, S. Hampshire, Sintered feldspar glass–ceramics and glass–ceramic matrix composites, Ceram. Int. 34 (8) (2008) 2037–2042.
[18] R.D. Rawlings, J.P. Wu, A.R. Boccaccini, Glass-ceramics: their production from wastes—a review, J. Mater. Sci. 41 (3) (2006) 733–761.
[19] M. Rezvani, B. Eftekhari-Yekta, M. Solati-Hashjin, V.K. Marghussian, Effect of Cr_2O_3: Fe_2O_3 and TiO_2 nucleants on the crystallization behaviour of SiO_2–Al_2O_3–CaO–MgO (R_2O) glass-ceramics, Ceram. Int. 31 (1) (2005) 75–80.
[20] M. Rezvani, B.E. Yekta, V.K. Marghussian, Utilization of DTA in determination of crystallization mechanism in SiO_2–Al_2O_3–CaO–MgO (R_2O) glasses in presence of various nuclei, J. Eur. Ceram. Soc. 25 (9) (2005) 1525–1530.
[21] M. Rezvani, V.K. Marghussian, B. Eftekhari Yekta, Crystal nucleation and growth rates: time–temperature transformation diagram, and mechanical properties of a SiO_2–Al_2O_3–CaO–MgO–(R_2O) glass in the presence of Cr_2O_3, Fe_2O_3, and TiO_2nucleants, Int. J. Appl. Ceram. Tec. 8 (1) (2011) 152–162.
[22] A.A. Omar, A.W.A. El-Shennawi, G.A. Khater, The role of Cr_2O_3: LiF and their mixtures on crystalline phase formation and microstructure in Ba, Ca, Mg aluminosilicate glass, Brit. Ceram. T. 90 (6) (1991) 179–183.
[23] A. Karamanov, P. Pisciella, M. Pelino, The effect of Cr_2O_3 as a nucleating agent in iron-rich glass-ceramics, J. Eur. Ceram. Soc. 19 (15) (2016) 2641–2645.
[24] L. Barbieri, C. Leonelli, T. Manfredini, G.C. Pellacani, C. Siligardi, E. Tondello, R. Bertoncello, Solubility: reactivity and nucleation effect of Cr_2O_3 in the CaO-MgO-Al_2O_3-SiO_2 glassy system, J. Mater. Sci. 29 (23) (1994) 6273–6280.
[25] K. Onuma, T. Tohara, Effect of chromium on phase relations in the join forsterite-anorthite-diopside in air at 1 atm, Contrib. Mineral. Petr. 84 (2–3) (1983) 174–181.
[26] K. Shih, T. White, J.O. Leckie, Spinel formation for stabilizing simulated nickel-laden sludge with aluminum-rich ceramic precursors, Environ. Sci. Technol. 40 (2006) 5077–5083.
[27] K. Shih, T. White, J.O. Leckie, Nickel stabilization efficiency of aluminate and ferrite spinels and their leaching behavior, Environ. Sci. Technol. 40 (2006) 5520–5526.
[28] Y. Tang, K. Shih, Y. Wang, T.C. Chong, Zinc stabilization efficiency of aluminate spinel structure and its leaching behavior, Environ. Sci. Technol. 45 (2011) 10544–10550.
[29] Y. Tang, S.S.Y. Chui, K. Shih, L. Zhang, Copper stabilization via spinel formation during the sintering of simulated copper-laden sludge with aluminum-rich ceramic precursors, Environ. Sci. Technol. 45 (2011) 3598–3604.
[30] G.A. Khater, Diopside–anorthite–wollastonite glass-ceramics based on waste from granite quarries, Glass Technol.-Part A 51 (1) (2010) 6–12.
[31] G.A. Khater, Glass-ceramics in the CaO-MgO-Al_2O_3-SiO_2 system based on industrial waste materials, J. Non-Cryst. Solids 356 (2010) 3066–3070.
[32] S.D. Yoon, J.U. Lee, Y.H. Yun, H.S. Yang, Chemical durability of wollastonite glass-ceramics derived from waste glass and sludge bottom ash, J. Ceram. Process. Res. 13 (1) (2012) 52–55.
[33] E. Mejia-Ramirez, A. Gorokhovsky, J.I. Escalante-Garcia, Crystallization behavior of glasses in the system of Na_2OCaO–MgO–Fe_2O_3–Al_2O_3–SiO_2 with high contents of nickel oxide, J. Non-Cryst. Solids 353 (4) (2007) 366–373.
[34] D. Dermatas, X. Meng, Utilization of fly ash for stabilization/solidification of heavy metal contaminated soils, Eng. Geol. 70 (3) (2003) 377–394.
[35] O. Malliou, M. Katsioti, A. Georgiadis, A. Katsiri, Properties of stabilized/solidified admixtures of cement and sewage sludge, Cement Concrete Comp. 29 (1) (2007) 55–61.
[36] D.L. Bish, S.A. Howard, Quantitative phase analysis using the Rietveld method, J. Appl. Crystallogr. 21 (2) (1988) 86–91.
[37] A.G. De la Torre, M.G. Aranda, Accuracy in Rietveld quantitative phase analysis of Portland cements, J. Appl. Crystallogr. 36 (5) (2003) 1169–1176.
[38] A.G. De La Torre, S. Bruque, M.A.G. Aranda, Rietveld quantitative amorphous content analysis, J. Appl. Crystallogr. 34 (2) (2001) 196–202.
[39] A.F. Gualtieri, V. Riva, A. Bresciani, S. Maretti, M. Tamburini, A. Viani, Accuracy in quantitative phase analysis of mixtures with large amorphous contents: the case of stoneware ceramics and bricks, *J. Appl. Crystallogr.* 47 (3) (2014) 835–846.
[40] A. Juhin, G. Calas, D. Cabaret, L. Galoisy, J.L. Hazemann, Structural relaxation around substitutional Cr^{3+} in $MgAl_2O_4$, Phys. Rev. B 76 (5) (2007) 054105.

[41] C.Z. Liao, K. Shih, W.E. Lee, Crystal structures of Al–Nd codoped zirconolite derived from glass matrix and powder sintering, Inorg. Chem. 54 (15) (2015) 7353–7361.
[42] B. Ravel, M. Newville, ATHENA, ARTEMIS, HEPHAESTUS: data analysis for X-ray absorption spectroscopy using IFEFFIT, J. Synchrotron Radiat. 12 (4) (2005) 537–541.
[43] A. Goel, D.U. Tulyaganov, V.V. Kharton, A.A. Yaremchenko, J.M. Ferreira, The effect of Cr_2O_3 addition on crystallization and properties of La_2O_3-containing diopside glass-ceramics, Acta Mater. 56 (13) (2008) 3065–3076.
[44] G.A. Khater, Influence of Cr_2O_3: LiF, CaF_2 and TiO_2 nucleants on the crystallization behavior and microstructure of glass-ceramics based on blast-furnace slag, Ceram. Int. 37 (7) (2011) 2193–2199.
[45] V.D. Tathavakar, M.P. Antony, A. Jha, The physical chemistry of thermal decomposition of South African chromite minerals, Metall. Mater. Trans. B 36 (1) (2005) 75–84.
[46] C.M. Jantzen, K.G. Brown, Predicting the Spinel–Nepheline liquidus for application to nuclear waste glass processing. part I: primary phase analysis, liquidus measurment, and quasicrystalline approach, J. Am. Ceram. Soc. 90 (6) (2007) 1866–1879.
[47] Y.C. Lin, S.L. Wang, Chromium(VI) reactions of polysaccharide biopolymers, Chem. Eng. J. 181 (2012) 479–485.
[48] Y.L. Wei, S.Y. Chiu, H.N. Tsai, Y.W. Yang, J.F. Lee, Thermal stabilization of chromium (VI) in kaolin, Environ. Sci. Technol. 36 (21) (2002) 4633–4641.
[49] D. Huang, C.H. Drummond, J. Wang, R.D. Blume, Incorporation of chromium (III) and chromium (VI) Oxides in a simulated Basaltic: industrial Waste Glass-ceramic, J. Am. Ceram. Soc. 87 (11) (2004) 2047–2052.
[50] US, EPA, Toxicity Characteristics Leaching Procedure (TCLP), Method 1311, U.S. Environmental Protection Agency, USA, 1992.